



# Review on integral stiffened panel of aircraft fuselage structure

Devi Chandra <sup>a</sup>, Y. Nukman <sup>b</sup>, Muhammad Adlan Azka <sup>c</sup>, S.M. Sapuan <sup>c,\*</sup>, J. Yusuf <sup>c</sup>

<sup>a</sup> Mechanical Engineering Department, Faculty of Engineering, Andalas University, Padang, 25163, Indonesia

<sup>b</sup> Department of Engineering Design and Manufacture, Faculty of Engineering, University of Malaya, Kuala Lumpur, 50603, Malaysia

<sup>c</sup> Advanced Engineering Materials and Composites (AEMC) Research Centre, Department of Mechanical and Manufacturing Engineering, Universiti Putra Malaysia, UPM Serdang, 43400, Selangor, Malaysia

## ARTICLE INFO

### Article history:

Received 28 May 2024

Received in revised form

31 October 2024

Accepted 20 November 2024

Available online 23 November 2024

### Keywords:

Integral stiffened panel

Buckling

Fatigue

Friction stir welding

Laser beam welding

## ABSTRACT

The increasing demand to decrease manufacturing costs and weight reduction is driving the aircraft industry to change the use of conventional riveted stiffened panels to integral stiffened panels (ISP) for aircraft fuselage structures. ISP is a relatively new structure in aircraft industries and is considered the most significant development in a decade. These structures have the potential to replace the conventional stiffened panel due to the emergence of manufacturing technology, including welding, high-speed machining (HSM), extruding, and bonding. Although laser beam welding (LBW) and friction stir welding (FSW) have been applied in aircraft companies, many investigations into ISP continue to be conducted. In this review article, the current state of understanding and advancement of ISP structure is addressed. A particular explanation has been given to (a) buckling performance, (b) fatigue performance of the ISP, (c) modeling and simulation aspects, and (d) the impact of manufacturing decisions in welding processes on the final structural behavior of the ISP during service. Compared to riveted panels, machined ISP had a better compressive buckling load, and FSW integral panels had a lower buckling load than riveted panels. Compressive residual stress decreased the stress intensity factor (SIF) rates, slowing down the growth of fatigue cracks as occurred in FSW and LBW ISP.

© 2024 China Ordnance Society. Publishing services by Elsevier B.V. on behalf of KeAi Communications Co. Ltd. This is an open access article under the CC BY license (<http://creativecommons.org/licenses/by/4.0/>).

## 1. Introduction

The majority of contemporary airplanes use curved aluminum alloy skin panels in their fuselage structure [1,2]. These panels are attached to stiffening members known as stringers and frames, which provide radial and longitudinal rigidity, respectively [3,4]. Usually, most skin panels have always been riveted to the stiffeners, which means many components require high cost and time consumption for the assembly. However, rivet stringer performs as crack stoppers with increasing fail safety design. The presence of rivet holes are stress raisers and can result in premature initiation of fatigue cracks [5–7].

The persistent demand for optimal cost-effectiveness in production and the advent of advanced manufacturing technology have sparked a renewed fascination with the use of large-scale integral metallic structures for aerospace applications [8–10]. Integral structure refers to the construction of skins and stiffeners as a

unified entity, which can be manufactured using extrusions, forgings, castings, or other methods. Additionally, these components can be joined together using welding or bonding [11,12]. It has the capacity to greatly reduce the need for multipart assembly and rivet joints. Additionally, it possesses the capacity to mitigate corrosion by eliminating vulnerable interfaces and can enhance structural efficiency by establishing uninterrupted load channels. Compared to conventional panels, Integral Stiffened Panel (ISP) offer additional benefits such as enhanced performance due to a smoother exterior surface resulting from fewer attachments and non-buckling skin, higher allowable stiffener compression loads due to the removal of connected flanges, and higher joint efficiencies under tension loads thanks to the use of integral doublers [13].

Several manufacturing technologies are used in the modern aircraft industry to craft ISPs that are partially integrated into the fuselage and wings of aircraft. At the moment, laser beam welding (LBW) and friction stir welding (FSW) are thought to be the most promising welding techniques. For a restricted design range on the A318 and A380 models, Airbus has used LBW in the manufacturing of pressure bulkhead skin-stiffener panels and fuselage, as shown

\* Corresponding author.

E-mail address: [sapuan@upm.edu.my](mailto:sapuan@upm.edu.my) (S.M. Sapuan).

in Fig. 1 [14–16]. It has already demonstrated benefits in overcoming the drawbacks of traditional riveted fuselages. The introduction of LBW technology into the fuselage of small passenger aircraft, like the ATR 42, is considerable, not just because of the potential for weight savings but also because of the need for quick manufacturing and cost control. Currently, complete stiffened panels with T-joints between the skin sheet and stringer are fabricated using the LBW technique. With two advantages over conventional riveting, this welding technology can produce extremely complex and competitive airframe parts: first, it reduces weight by eliminating the need for material to be added as rivets and metal sheet overlap; second, it can produce parts at a high rate because LBW is very fast [17,18].

The manufacture of airplane structures extensively uses FSW. Aluminium has experienced the most rapid progress since the introduction of FSW in the early 1990s due to its low melting point, high heat conductivity, and ductility [20,21]. Boeing 747 cargo initially implemented it on its nose barrier [22]. Eclipse Aviation utilized FSW to manufacture the fuselage and wing of the Eclipse 500 business jet [23]. Boeing invested \$15 million in FSW to weld the booster core tanks for the Delta line of space launch vehicles. This investment was the first instance of FSW being used for manufacturing in the United States [24,25]. Furthermore, according to Majeed et al. [26], Boeing company analyzed 60% cost and 26% production time reduced in designing FSW fabricated Delta II and Delta IV for satellite launch vehicles. Fokker Aviation used FSW to connect the Ariane 5's motor thrust frame. This frame consisted of 12 sheets reinforced with stiffeners [27]. FSW floor structure was also utilized by the freight aircraft C130). Subsequently, this technique has been used to produce a large number of goods, some of which include sheet structures with stiffeners. In contrast to traditional fusion welding, FSW is a solid-state procedure that uses frictional heat generated between a rotating tool and the material to be welded. This reduced heat input helps to lessen residual stress from the welding process and structural distortion. Several types of joints, including fillet, T-butt, butt, and lap joints, can be joined by FSW. According to the main research on FSW joint, it is possible to achieve minimal distortion and high efficiency lap joint of aluminium panels [28]. The FSW technique, known for its superior strength, non-melting properties, and ecologically benign characteristics, has demonstrated cost savings in several applications and facilitated the creation of innovative product forms. Fig. 2 shows the schematic process of FSW.

Although numerically controlled machinery has been well

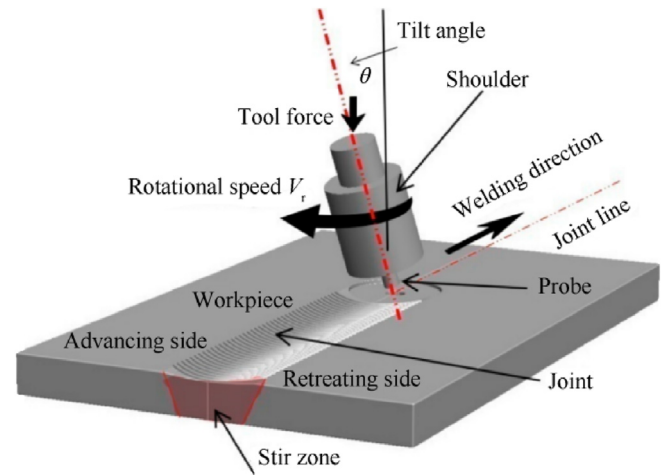


Fig. 2. A schematic of the FSW process [29].

established, the introduction of high-speed machining (HSM) for manufacturing structural components from thick aluminum plates has several benefits [30–32]. These benefits include reduced production time, uniform results, and the ability to fabricate thin-walled components [33]. Cost analyses further showed that the panel constructed from a machined plate provided a cost reduction of 61% compared to the standard conventional panel [34]. Although the emergence of ISP has provided many advantages over the differential panel, the disadvantages need to be addressed. When a skin crack intersects an ISP, it propagates continuously in both the skin and the stringer. The crack is unable to divert from its original crack path. The residual stress, residual distortion, and degradation material due to the welding method affect the stability performance and geometry tolerance of the panel structure [35]. Furthermore, the LBW technique presents crack-free connections with low porosity [36,37], which ultimately leads to good mechanical performance of the welded joint, which is difficult to achieve [38–40].

Moreover, there should be a more thorough investigation into the creation of numerical or analytical formulations that can accurately forecast the global and local buckling loads and the ultimate strength or collapse load of the structure in both the elastic and elastoplastic ranges. Investigations into ISPs have been a fascinating topic for many years. Many researchers have devoted significant resources to studying panel structures' responses. Nevertheless, understanding every facet of behavior as a whole continues to be challenging due to its intricate nature and the multitude of variables at play. This review paper offers a comprehensive overview of the current understanding and advancements in the field of integral stiffened structures. The study provides a thorough explanation of the buckling and fatigue of integral fuselage structures, the modeling and simulation aspects, and the impact of manufacturing decisions in welding processes on the final structural behavior of ISP during service. This paper aims to broaden the researcher's knowledge, enabling them to optimize their research on the ISP of aircraft fuselage structures.

## 2. Buckling of integral fuselage structure

Buckling is a crucial and frequently decisive factor in the design of airplane constructions [41,42]. Essentially, the buckling phenomenon is influenced by the mechanical characteristics of the material, contact conditions, and structure geometry. The buckling of a fuselage panel results in localized displacement and stress

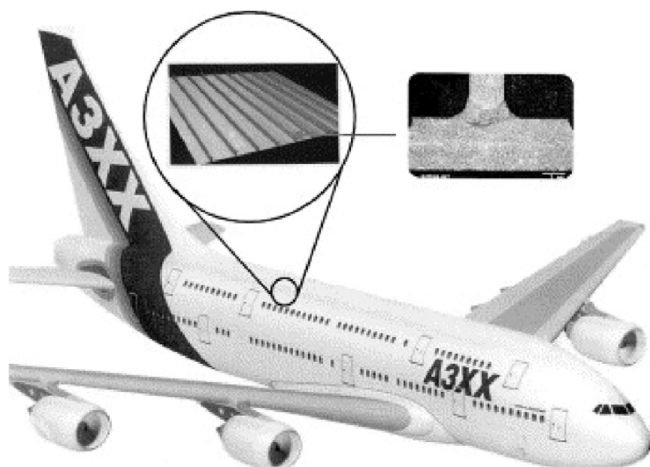


Fig. 1. Future application of laser beam welded structures in the aircraft industry [19].

gradients that exceed those found in an unbuckled panel [43,44]. Performing an examination of buckling initiation and growth has gotten challenging because of the intricate effects of the regulating parameter. Frequently, it has been noted in instability occurrence that little alterations in the parameters can lead to very diverse buckling behavior. As a result of these challenges, the buckling analysis has often been carried out individually for each specific scenario. Buckling research on aircraft ISP specifically focuses on topics such as imperfections and residual stress in real structures, the impact of different boundary conditions, the application of computerized modeling and numerical buckling analyses in the stability model of complex panel structures, and the buckling of panels in local or non-uniform loads and localized compressive stresses. In recent decades, researchers have studied a wide range of buckling problems with ISP. Finite element (FE) analysis and other computer approaches have been employed to minimize the necessity for testing and conducting parametric design studies [45]. On the other hand, some experimental methods in both laboratory and full scales have also been conducted to validate the computational results. Several publishing works undertaken to focus on the buckling of ISP in both computational and experimental methods are presented below.

Aalberg et al. [46] analyzed the flexural buckling of extruded-welded aluminum alloy 6082 T6 ISP. Two extruded panel types, i.e., open section (L-shaped) stiffeners and closed section stiffeners as shown in Fig. 3 are fabricated by mean MIG welding and FSW, respectively. The tests identified two main types of deformation: collapse due to stiffener tripping (ST) or flexural buckling (FB) of the full panel, resulting in either positive or negative out-of-plane displacements ( $w$ ). According to the test results, the panels failed in stiffener tripping, flexural buckling paired with local plate buckling, and total flexural buckling. The stiffened panel's mode of failure had a notable impact on the panel response in the post-buckling range in terms of axial load versus shortening, with stiffener tripping being the least preferred because of its rapid fall in resistance beyond the ultimate load.

Lockheed-Martin Space Systems conducted an investigation for NASA where they designed, manufactured, and experimentally tested a large-scale FSW panel made of 2090-T83 aluminum-

lithium (Al-Li) alloy. The aim of this investigation was to analyze the suitability of using FSW as an alternative to conventional rivet fastening for constructing the dry bay of launch vehicles [47]. Both the FSW panel and a regular riveted panel underwent compression testing to failure. The study examined panel samples with multiple stiffeners in a hat section profile. Large initial geometric defects and initial skin buckling at loads much below projected values were seen in both the riveted and FSW panels [48]. Scientists identified a number of variables, such as distortion, geometric flaws, and diminished weldment qualities, to explain this behavior. It was determined that the FSW panel performance was significantly influenced by distortion. The riveted panel's ultimate load strength reached a greater value than anticipated, whereas the FSW panel's failure load was 5% lower than expected due to welding flaws (the welded panel had a 20% lower load of failure than the identical riveted panel). The FSW panel did not experience a catastrophic failure but rather exhibited ongoing deformation after reaching the maximum load, in contrast to the riveted panel, which had a severe failure at the same point.

Murphy et al. [49] assessed the conventional and FE analysis processes for the buckling and crippling strength analyses of friction stir welded skin-stringer joints panel. The conventional analysis methods were done based on the conventional airplane panel analysis technique as found in the NASA Astronautics Structures Manual or the ESDU Structures Sub-series. Meanwhile, the FE analysis method examined the initial buckling load, initial buckling modes, and crippling failure load of three kinds of skin stringer weld joint model idealizations. The study was verified using a single test specimen of a stiffener crippling, which consisted of a Z-section stringer stiffener made from a 7075-T76511 extrusion and a flat skin base made from 2024-T3. In all analyses, the authors did not consider welding effects on material properties and resultant residual stresses. The authors came to the conclusion that conventional buckling conducted may be taken into consideration when analyzing the crippling behavior of FSW stiffened panels. To take into consideration the weld joint geometry, however, normal stiffened panel buckling analysis methodologies must be modified. Furthermore, the crippling behavior may be accurately modeled using non-linear FE analysis techniques; yet again, this requires an

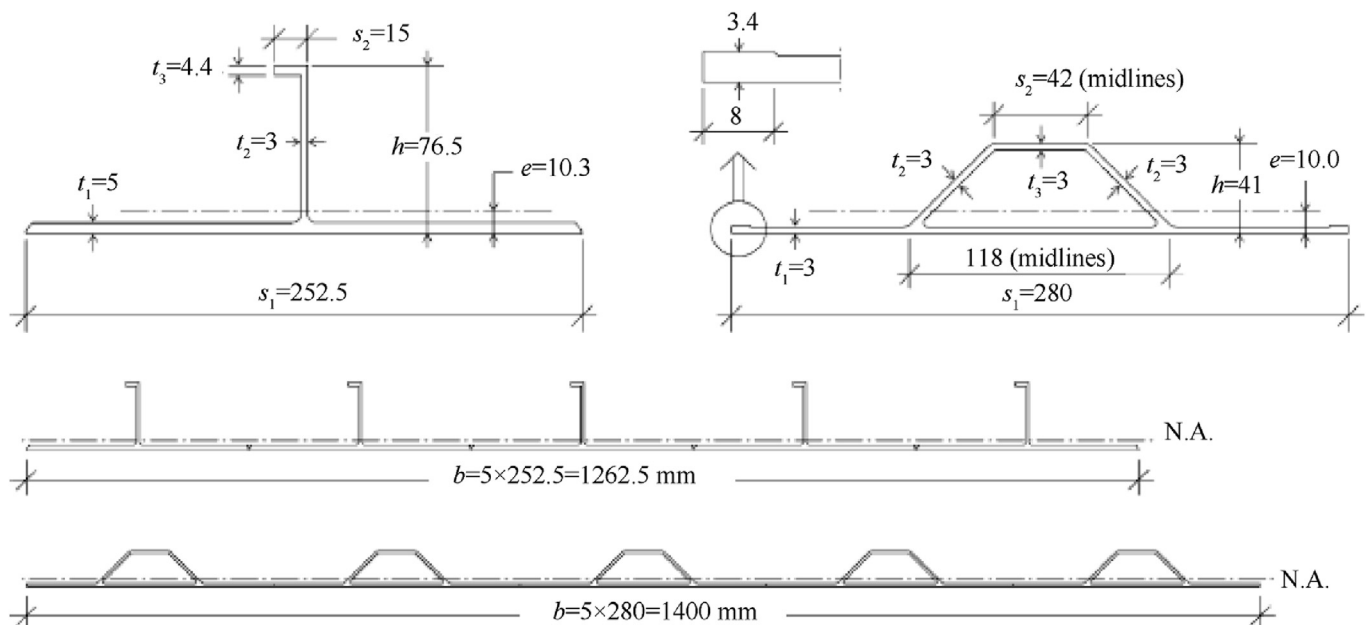


Fig. 3. Cross-sectional geometry of extruded profiles and cross-sections of panels containing five extruded profiles joined by welding [46].

accurate representation of the weld joint geometry and the contact conditions at the joint interface.

Murphy et al. [50] characterized the primary methods by which FSW assembly processes impact the buckling performance of stiffened panels. Empirically verified FE models have demonstrated that the intensity of residual stresses caused by welding and the resulting shape distortions have a notable impact on the early buckling of a stiffener FSW panel's skin. Moreover, they found that the post-buckling or collapse behavior was less affected by the applied process effects and the magnitudes of these effects when compared to the initial buckling behavior.

Weimin et al. [51] conducted a comprehensive study to examine the structural behavior of a curved build-up panel and an integrated panel when exposed to a uniform axial compression force. The investigation involved both experimental and numerical analyses. The panel test specimen was constructed with 3 stringers and 2 frames, and the panel skin was constructed using a 2024-T4 aluminum sheet, while the stringer and frame were constructed using 7075-T62 aluminum Z sections. The frames were securely attached to the panel's skin using aluminum shear clips, and the integrated panel and the build-up panel had identical overall dimensions and weights. The skin-stringer panel was manufactured by machining a single plate of 2024-T4 aluminum alloy, while the frames were constructed from Z-shaped sections of 7075-T62 aluminum alloy and securely attached to the panel skin using mechanical fasteners. The PATRAN code was utilized to do a nonlinear FE analysis. The simulation included elements such as significant displacement, the plasticity of the material, and contact interactions between several deformable bodies. The experiment and FE analyses indicated that when the stress on the skin exceeded the yield limit, it caused damage to the integral panel under a post-buckling load. Additionally, when buckling waves crossed the stringers at an oblique angle, it resulted in damage to the build-up panel. Comparisons between integral panels and build-up panels revealed that integral panels had a higher compressive load capacity. Furthermore, the critical compressive load of integral panels rose by 18.4% in comparison to build-up panels.

Yoon et al. [52] employed numerical analysis to determine the buckling characteristic of an FSW ISP structure. The researchers used the Ramberg-Osgood constitutive model in the Abaqus FE code to find the material's inelastic range for making two and three types of stiffeners. They deduced that the weld's presence resulted in a decline in the maximum buckling force by 3%–10% since the reduced material behavior in the weld zone. The drop in the 2-stiffener ISP portion was greater than that in the 3-stiffener ISP configuration of the closer weld spacing.

Khedmati et al. [53] examined how various factors, such as the thickness of the plate, the conditions of boundary, the geometries of the stiffener, as well as the width of welding HAZ and residual stress, affect the post-buckling behavior and ultimate strength of welded stiffened aluminum alloy plates subjected to a combined axial compressive and lateral pressure load. They used the nonlinear FE method for their analysis. The ANSYS code was used to examine three types of stiffeners (weak, medium, and heavy) with three different geometries (flat, angle, and tee) in each type. The analysis considered both material and geometric non-linearities. The researchers discovered the following: (i) when subjected to low lateral pressure, the panel collapsed due to axial compression in a mode where it was simply supported; (ii) as the lateral pressure load increased, the collapse mode shifted to a clamped mode; (iii) a rise in the width of the HAZ resulted in a decrease in ultimate strength, following a bilinear trend; and (iv) the presence of welding residual stress caused a reduction in ultimate strength, which was influenced by the amount of type stiffener and the value of lateral pressure.

Neto et al. [54] examined the primary distinctions in the strength characteristics of local buckling on FSW and rivet-stitched panels. The FE commercial code NASTRAN was used to model and analyze a series of one-bay panels with varying quantities of evenly spaced longitudinal Z-stiffeners. The panel skin was composed of aluminum alloy 2024-T3, while the longitudinal stiffeners were built from aluminum alloy 7050-T3511. Three straightforward processes were implemented for the FSW join. Initially, the TMAZ width was assumed zero, and the weld was treated as a straight line. Furthermore, the nodes in the weld joint area between the skin and stiffener were linked together using the RBE2 rigid element. The contact conditions between the stiffener flange and unwelded skin were represented using a uniaxial linear gap method. The skin rivet joints utilized CELAS2 spring elements to model the transverse and axial joint stiffness of the rivet. These spring elements link the flange center node to the skin's projection node. Regarding local buckling, it was determined that the disparities in local buckling strength between FSW and riveting stiffened panels were insignificant when taking into account stiffened panels without imperfections and the extent of extension or degradation in the material's HAZ. Nevertheless, the process of skin welding resulted in residual stress, which was critical for determining the FSW's true local buckling strength.

Caseiro et al. [55] used three different optimization techniques—Hybrid Differential Evolution Particle Swarm Optimization (HIDEPSO), Levenberg-Marquardt (LM) model, and Simulated Annealing (SA) model to optimize an ISP that was subjected to buckling forces. ABAQUS was used to do the buckling analysis, which involved Ramberg-Osgood and the Riks methods. The cross-sectional area values obtained by the SA and HDEPSO algorithms were smaller, which improved the ratio between the structural weight and the buckling load limit. However, with fewer function evaluations, the LM method produced a satisfying result.

To ascertain the effect of experimental errors, Shah et al. [56] analyzed the disparities between the FE model and research findings for a welded fuselage panel that was exposed to uni-axial compression. The researchers used FE models to analyze the consequences of employing various boundary conditions for simulating the experimental configuration. These models included shell elements, as well as a mix of shell and solid elements. In addition, they employed a newer version of the ABAQUS software to accurately simulate the panel's shape. The researchers determined that the latest version of ABAQUS yielded superior results in terms of stiffness and failure load. Moreover, the inclusion of solid components closely corresponded to the stiffness values of the FE model, as observed in the experimental results.

### 3. Fatigue of integral fuselage structure

When a structure is repeatedly loaded, fatigue is the process that leads to an early failure [57,58]. It is described as a gradual failure phenomenon that advances when cracks begin to form and spread to an unstable size [59,60]. Since it indicates how durable an aircraft structure and the growth of fatigue crack rate is a crucial criterion. Numerous factors, including material qualities, manufacturing quality, chemical environment, and stress history, might influence fatigue failure. Stress studies of cracked aircraft parts, our knowledge of how fatigue and fatigue-crack growth happen in metals, and our ability to guess the remaining strength of aircraft structures that are still together after a lot of fatigue damage have all come a long way from 1969 [61].

Integral fuselage structures must be developed using damage tolerance principles to withstand various forms of damage during their lifespan without affecting their structural integrity. The utilization of joining technologies such as FSW and LBW in structures

generates residual stress fields that impact their fatigue characteristics. The residual stresses occur because of the temperature gradients produced by the welding process. In the FSW process, residual stresses are induced not only by the thermal field but also by the mechanical action involved. Multiple investigations have been carried out to ascertain the fatigue characteristics of the integrated fuselage structure. Recent advancements in computer technology have facilitated more precise stress analyses on three-dimensional crack configurations, more authentic simulations of fatigue and fatigue cracking in structural components, and the application of more intricate fracture mechanics principles to assess the strength and fail-safe capabilities of aircraft structures. The subsequent segment described the investigation into the fatigue of ISP areas.

The NASA Integral Airframe Structures program examined the viability of employing integrally stiffened fabrication for fuselage structures in transport aircraft [62,63]. The aim of the research was to evaluate that integrally stiffened fuselage panels made from Al7050 and Al7475 plates perform at least as well as traditional structures in terms of weight, structural integrity, and cost-effectiveness. This was done through pressure, compression, and fatigue tests. The panel's residual strength testing indicated that it could withstand a pressure range of 9.7–9.89 psi. The test findings also indicated that the panel manufactured from 7475-T7351 had slow crack propagation. Despite the panel design not being fully optimized and lacking comprehensive structural criteria, the panel's crack arrest performance showed great promise.

Zhang et al. [7] determined the impact of welding residual stress on the lifespan of fracture development in welded ISP using experimental and computational methods. The study utilized two separate design configurations. Initially, a panel consisting of two strings was used to investigate and confirm the effects of fatigue through experimental studies. Furthermore, a panel consisting of nine strings was compared to a riveted panel with the same geometry. The stress intensity factor (SIF) was measured using the FE method with the MSC NASTRAN software package. The applied SIF range ( $\Delta K$ ) was then modified by the effects of cyclic plasticity (crack closure) and welding residual stresses through the argument of the effective stress-intensity-factor range ( $\Delta K_{\text{eff}}$ ). According to the study, cracks originating from the weld joint exhibited accelerated growth because of the occurrence of residual tensile stresses in the fusion and HAZ. This showed that the rate of crack propagation was higher in machined stringer panels compared to integrally machined stringer panels. Moreover, the simulation results demonstrated that integrally machined or welded stringers were more efficient than riveted stringers in minimizing SIF at the connection area between the stringer and the skin. Integral panels exhibited a reduced crack propagation rate near the outer stringer compared to riveted panels when a skin fracture was approaching. The welded integrated panel had the highest fatigue crack development life but demonstrated the worst failure safety characteristic as a result of an unstable crack that occurred after the failure of two external stringers. The slower rate of fracture propagation in the welded panel could be associated with the compressive residual strains induced by the welding process near the skin doublers. Hence, when a fracture was initiated outside the HAZ and grew between the stringers, the pace at which the crack grew diminished.

Burford et al. [22] investigated the rates at which fatigue cracks grew in AA2024-T3 sheets that were connected to AA7075-T6 stiffeners using FSW. Friction stir panels were produced employing both continuous FSW and sweeping friction stir spot welding (FSSW). Edge crack panels with continuous FSW joints generally propagated fatigue cracks into the parent material, moving away from the stiffeners. The raised thickness of continuous FSW joints,

along with the reinforcement provided by the connected stiffener, were factors that contributed to the reduction in stress levels. Panels created with rivets and swept FSSW connections showed cracks aligned with the joint line. The crack propagation rates in riveted panels increased as the crack approached the riveted joints. Conversely, the speed at which fractures spread in panels joined using FSSW decreased significantly as the fractures approached the joints formed by the swept-spot welding. The research showed that the swept FSSW method created helpful residual stresses that stopped fatigue fractures from spreading along the joint line.

Brot et al. [64] performed a thorough examination of crack growth in the A2024-T351 two-stringer ISP. A FEM was constructed using StressCheck p-version software. To calculate the SIFs for modes 1 and 2, this software used linear elastic fracture mechanics (LEFM). A crack growth analysis was conducted using NASGRO version 5 software based on the stress-intensity findings obtained from StressCheck. The analysis focused on two stages of crack propagation: the initial stage involved the formation of the crack on the material's surface prior to reaching the integrated stiffener. In the second phase, there were two distinct fracture paths: one on the skin and another on the stiffener. The numerical results were compared to the empirical test results. In the experiment, three panels, each with a two-stringer structure, were subjected to crack growth testing. Based on the results of the FE and experiment tests, it was determined that ISP generally lacked strong damage-tolerance performance. The light integral stiffener provided minimal resistance to the crack's propagation. When the integral stiffeners had a significant weight, the failure of any stiffener significantly sped up the propagation of cracks in the panel. The researchers also utilized and evaluated composite material strips that were adhered to the panel. As a result, the panel's resilience improved significantly.

Merati et al. [65] manufactured and tested five different weld configurations of friction stir welded AA7075 stringer-AA2024 skin lap joints panel: single pass continuous, double pass continuous, double pass discontinuous, (DPD), DPD+plugged (rivet), and conventional riveted joints. The authors concluded that the fatigue lives of different FSWs were dependent on the weld setting. The result showed that the double pass welds FSW had the best fatigue performance and FSW performance was more consistent than riveting.

Llopart et al. [66] performed numerical and experimental works to determine the influence of stringer geometry on SIF  $K_1$ . Several stringer geometries involved baseline-stringer, J-stringer, hat stringer, nose-stringer, round-stringer, triangle-stringer, keyhole-stringer, and double flange-stringer were modeled and analyzed using StressCheck code. A comparison of the SIF value for all stringer versus crack length is shown in Fig. 4. The depicted figure demonstrates that the doubler flange stringer exhibited the most notable enhancement in SIF, increasing from 6% to 18%. Additionally, it was evident that the geometry of the stringer only had a major impact on crack propagation when the crack was in close proximity to the stringer.

Castro et al. [67] examined the fatigue behavior of AA6056 ISP using FE analysis and experimentation analysis. The test panels are manufactured by means of HSM, LBW, and FSW. Stiffened panels were fatigue tested at an ultimate stress of 80 MPa with  $R = 0.1$  and at an ultimate stress of 110 MPa with  $R = 0.5$ . The HSM sample exhibited the shortest fatigue life for both  $R$  values. In contrast, the PWHT-T6 samples tested in the LBW2 configuration (butt joint) exhibited longer fatigue lifetimes for both  $R$  ratios. The FSW sample evaluated at an  $R$ -value of 0.1 exhibited a fatigue life comparable to that of the LBW2 as-welded sample. At an  $R$ -value of 0.5, the FSW sample exhibited superior performance compared to the LBW1 PWHT-T6 sample but inferior performance compared to the LBW2

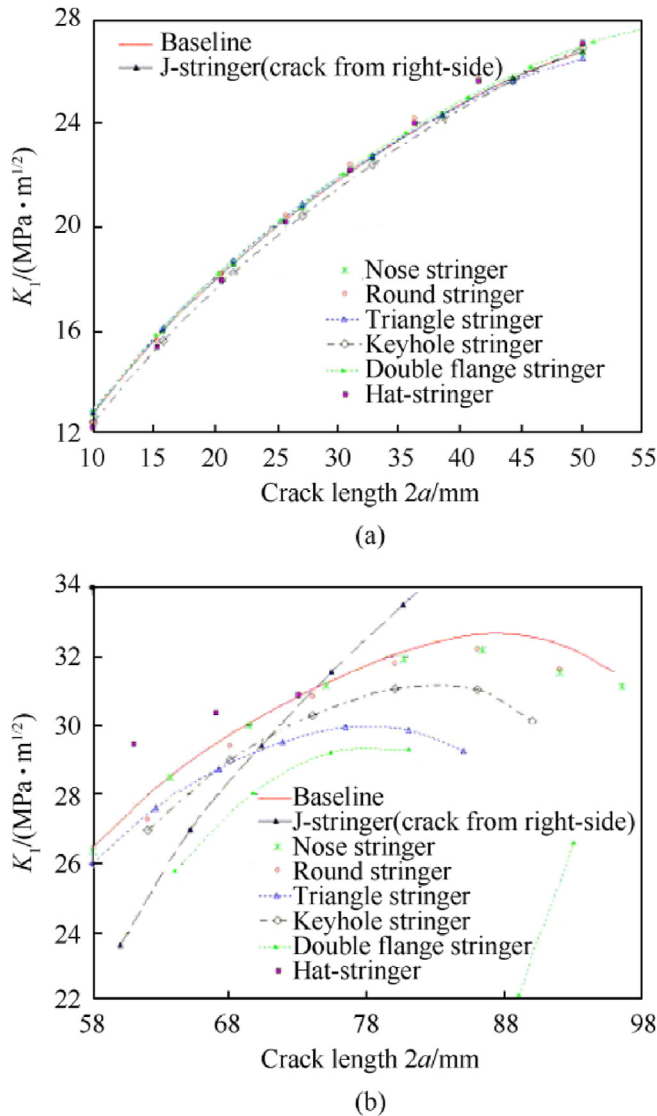


Fig. 4. SIF-values for all stringer cross-sections versus crack length [66].

as-welded sample. Upon examination of all samples, it was determined that the crack arrest feature, characterized by a decline in crack growth rate, was not significant. This lack of significance was likely attributed to the narrow width of these samples. However, if the stiffeners get shattered, the remaining lifespan of the sample is minimal.

Tavares et al. [68] conducted research that utilized LEFM principles to ascertain the fatigue life of integral structures including residual stresses. The work utilized ABAQUS finite element models, the Modified Virtual Crack Closure Technique, and the J-integral technique to measure the SIF of cracked stiffened panels subjected to mode I loading. After performing this calculation, the NASGRO law was employed to ascertain the fatigue lifespan of the panel, taking into account the impact of residual stress. This law allows us to model the effect of the load ratio variation and includes the description of the three regions of the fatigue growth crack curve. The author's conclusion was that HSM panels, which assumed the absence of residual stress, had a shorter lifespan. However, the FSW panels had a longer lifespan due to the residual compressive stress field situated in the core of the panel. This stress field effectively slowed down the propagation of cracks. The findings indicated that

the occurrence of residual compressive stresses had a positive impact on the fatigue durability of structures. Nevertheless, if a fracture is initiated in a region with tensile residual stresses, it will propagate at an accelerated rate.

Labeas et al. [69] developed a numerical methodology based on three-dimensional FE Analysis by ANSYS to calculate the SIFs at cracks in the HSM panel and LBW panel. The cracked stiffened panel is analyzed with applied Paris law to calculate crack propagation using three SIFs  $K_{max}$ ,  $K_{min}$ , and  $K_{aver}$ . The numerical thermo-mechanical simulation was used to measure the residual stresses due to the LBW process. These residual stresses were then incorporated into the fracture mechanics analysis to evaluate the impact of the residual stress field on crack propagation. The fatigue crack propagation (FCP) results were compared to the corresponding experimental data acquired under the DaToN Project. The findings in Figs. 5 and 6 demonstrate that residual stresses resulting from LBW caused a decrease in SIF values. This was consistent with the experimental findings of LBW panels, which demonstrated reduced FCP rates compared to the corresponding HSM panels. The reason for this discovery could be traced to the fact that the residual stress levels in the region where the crack fronts located were mostly compressive during the period of FCP.

In their investigation, Nesterenko et al. [70] conducted a comparison of integrated and riveted panels. The study revealed that the fatigue crack growth durations were nearly identical in both panels, regardless of whether the initial damage was a skin crack located below a fractured core stringer or between adjacent stringers. This statement holds true under the condition that both the integrated and riveted panels were constructed using the same material, in this case, the D16 alloy. A riveted structure panel had a greater residual strength than an integrated structure panel. After examining their work, it was noted that the outside stringers in both types of panels were allowed to fail once the skin crack had moved past the stringer. As a result, there was only a slight difference between the two panels in terms of fail-safety (two-bay fracture) and damage tolerance. Riveted stringers composed of high-strength alloys, such as the commonly utilized 7075-T6 alloy, were expected to stay undamaged even if a break in the outer layer propagated.

Adeel et al. [71] studied the crack propagation properties of the ISP and the conventionally stiffened aluminum panel using fracture mechanics and FE analysis. The two types of stiffened panels were studied using the FE analysis software ANSYS, with the skin and stringer modeled using the SHELL181 4-node element. The rivets

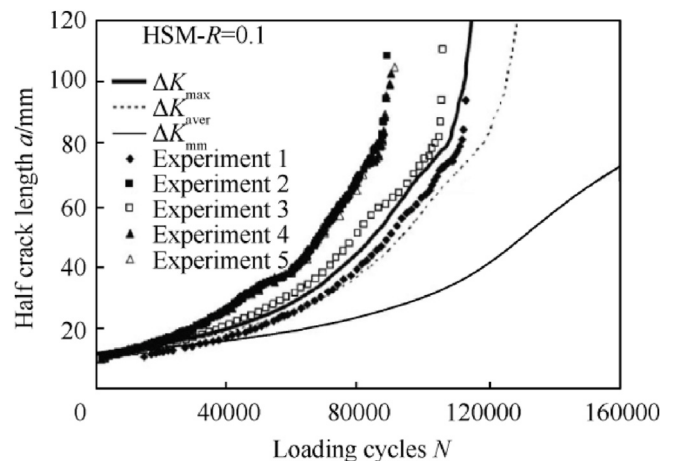


Fig. 5. Comparison of calculated crack propagation with experimental measurements [69].

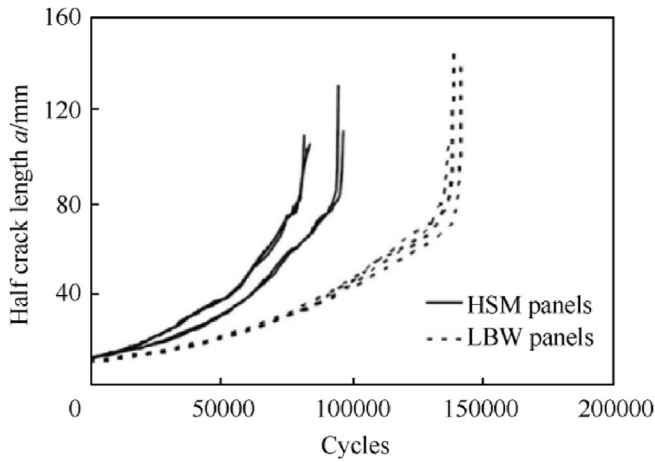


Fig. 6. Experimental fatigue crack propagation in HSM and LBW stiffened [69].

were simulated in ANSYS using the spot weld features, which relied on the internal multipoint constraint (MPC) method. The study generated a graph comparing SIF ( $K_I$ ) to half crack length ( $a$ ) for both types of stiffened panels and the unstiffened panel, as depicted in Fig. 7. Fig. 8 shows the relationship between half crack length and the rate of FCP ( $da/dn$ ) which determined using the Paris law. The study indicated that integral stiffening led to a larger SIF compared to conventionally stiffened panels when the crack tip moved across the stringer. Additionally, the ISP exhibited less damage tolerance than the riveted stiffened panel.

Uz.V et al. [72] conducted a comparison of the fatigue fracture propagation characteristics between LBW Al2139-T8 stiffened panels and panels with crenellations, as depicted in Fig. 9. Experiments were conducted on panels, including crenellations, to investigate the phenomenon of FCP in fractures that spread at a right angle to the welded stringers. The tests were carried out under two different loading conditions: steady amplitude and spectrum loading. An initial notch of 64 mm in length and 0.3 mm in width was formed in the center of both the stiffened panels and the base metal panel employing the electro-discharge machining

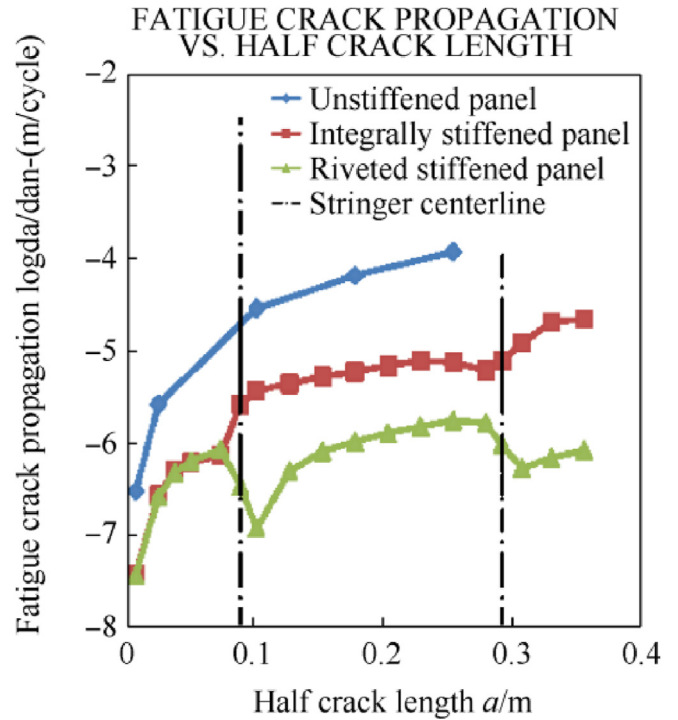


Fig. 8. FCP vs crack length [71].



Fig. 9. Schematic representation of a crenellated test panel [72].

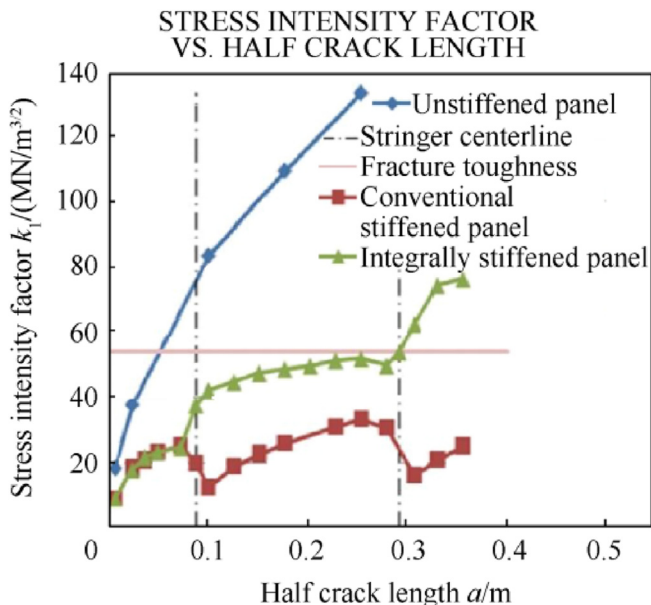


Fig. 7. SIF vs half crack length [71].

(EDM) method. The middle stringers were severed on the reinforced panels, including this incision. In Fig. 10, it can be seen that the crenellated panel greatly increased the overall lifespan

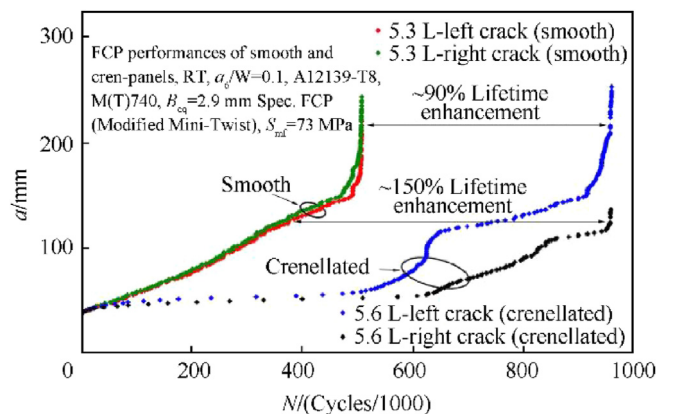


Fig. 10. Comparison of a vs. N curves of reference and crenellated panels under spectrum loading [72].

compared to the case where the amplitude loading stayed the same. The overall lifetime enhancement increased from approximately 65% under steady amplitude loading to a range of 90%–150% with spectrum loading. The novel panel form with crenellations had significantly longer fatigue lives than regular LBW panels.

Augustin et al. [73] used a computer simulation to show how fatigue cracks form in an HSM Al 2024-T351 ISP loaded with both constant amplitude and spectrum. The SIF calculations for cracks in the skin and stiffeners, acquired from MSC Patran/Nastran, were inputted into the NASGRO crack growth analysis tool. The crack closure method (CCT) was utilized in this process. The SIF calculation demonstrated a substantial decrease in growth when passing through the stiffener. NASGRO examined three crack propagation models: non-interaction, Willenborg, and strip yield. To make sure the crack growth simulation was correct, researchers tested and analyzed a basic CCT specimen and a two-stringer HSM panel specimen. The Willenborg and strip yield models demonstrated the highest accuracy in estimating the fatigue crack growth life, with an error rate of less than 9%, according to the test results. When compared to experimental results, these models demonstrated the highest level of precision in predicting fracture propagation for the CCT specimen model. The HSM panel with two strings accurately forecasted crack growth, with a maximum deviation of around 25%.

Lemmen et al. [74] examined how the weld nugget zone, TMAZ zone, and HAZ zone affect the fatigue start behavior of the FSW joint AA2024-T3 for various weld orientations. The specimen was fabricated by welding four sheets, each with a thickness of 2.5 mm, together. The welds were spaced 150 mm apart for the T-L specimens. On the other hand, for the L-T specimens, several sheets measuring 60 mm in width and 600 mm in length were welded together, as illustrated in Fig. 11 holes with a diameter of 1 mm, were drilled at specific locations according to the hardness profile. The sample was obtained by severing the strip from a welded sheet and then precisely shaping it to a width of 50 mm. The fatigue test was examined using constant amplitude loading with a stress ratio ( $R$ ) of 0.1 and a frequency of 10 Hz. The potential drop method (PDM) was employed to identify the onset of cracks and quantify the length of cracks at intervals of 2500 cycles. Figs. 12 and 13 depict the fatigue initiation test results for both the T-L test specimen and the L-T test specimen. There were no notable differences between the S-N curves for several points in the T-L test specimen's weld. Unlike the T-L test results, the findings indicated significant disparities in fatigue initiations across several locations. The researchers determined that the disparities reported in the fatigue

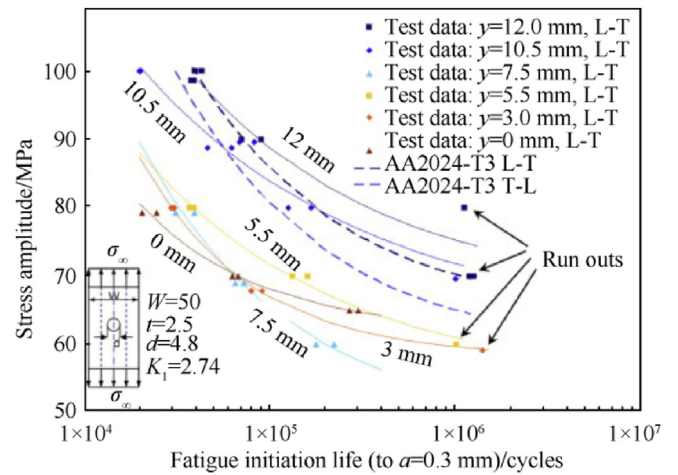


Fig. 12. Results from the L-T FI tests [74].

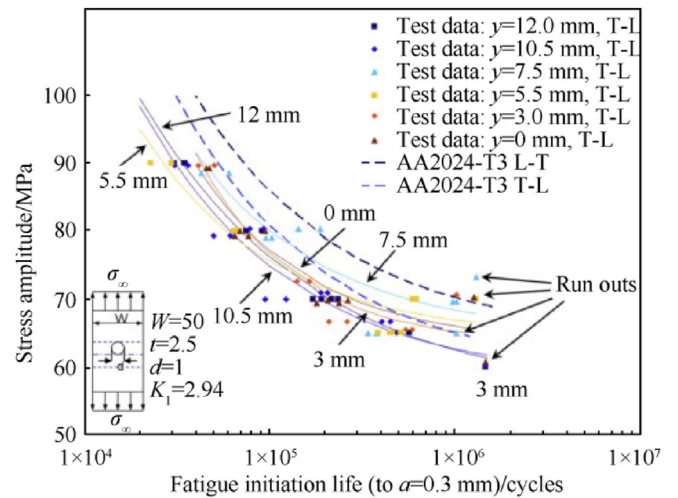


Fig. 13. Results from the T-L FI tests [74].

initiation test results between the L-T and T-L orientations were associated with the residual stresses present in the weld.

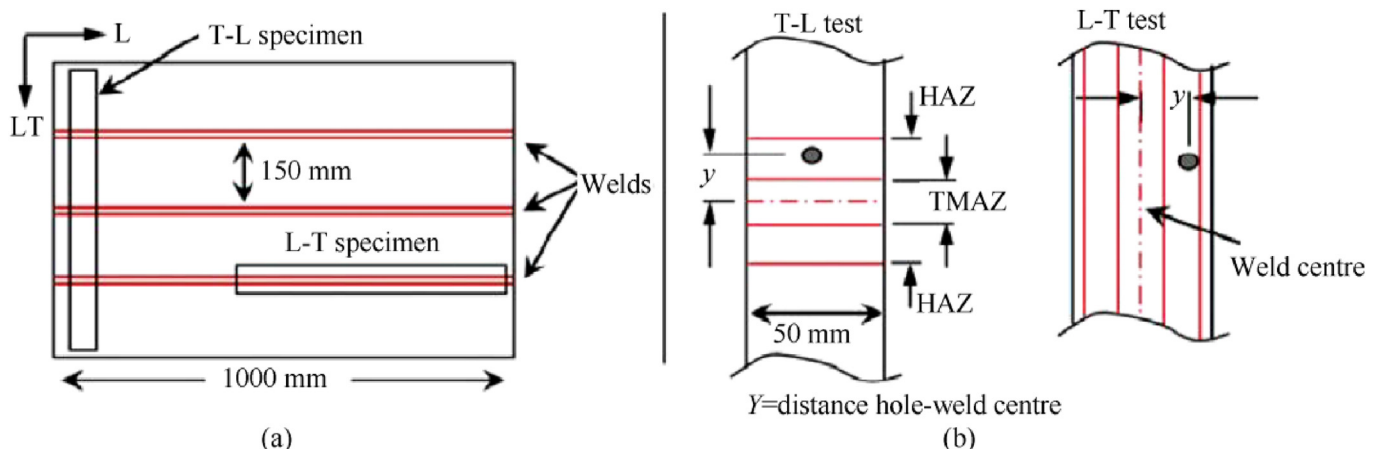


Fig. 11. (a) Example of how specimen is taken from the welded sheets; (b) Details of how welds and holes are situated in the different test specimens [74].

#### 4. Modeling and simulation aspects

The research by Paulo et al. [75] represented that shell FE models can precisely forecast the behavior of stiffened panels under compressive loads, especially at the ultimate load level, in the occurrence of elasto-plasticity. The eventual load was forecasted with remarkable precision, notwithstanding the imperfect connection between numerical simulations and experimental data. Both evaluated models exhibited significant sensitivity to initial imperfections, whether related to shape or magnitude. Maximum variances of 14.9% and 22.4% were recorded for types TR and L, respectively, using the same 2 mm magnitude with differing forms. The escalation in the extent of defects markedly affects the trend of ultimate load levels, contingent upon the selected shape of the imperfections. The majority of initial imperfections shapes exhibited a reduction in ultimate load as their magnitude grew; however, several shapes demonstrated an opposing tendency. The imperfect shapes derived from the prior studies devoid of imperfections at the collapse moment facilitated the identification of the minimal ultimate load values, or approximations thereof, for a specified imperfection magnitude. This kind of flawed form resulted in ultimate load fluctuations of up to 14.4% within a range of magnitude (0–2 mm). The use of a material with heat-affected characteristics in the HAZ did not substantially influence the ultimate load value relative to models that utilized the original plate material properties in the same region. Consequently, when subjected to compressive loads, an accurate ultimate load prediction must be preceded by a thorough evaluation of the geometric defects included in the original model.

Paulo et al. [76] analyzed the influence of residual stresses on the plate subjected to compressive load strength. The contour method was employed to characterize the residual stress fields in FSW, facilitating a detailed mapping of longitudinal residual stresses within the welded plate cross-section. The research indicated that residual stresses reduce the plate's collapse load in comparison to stress-free models, influenced by the length of the plate and the extent of geometrical imperfections. Geometrical imperfections had a substantial impact on plate behavior and collapse load, where a rise in the magnitude of imperfections leads to a reduction in collapse load. Furthermore, Paulo et al. [77] assessed a shell-based FE model designed for simulating the transient thermal field and stress-strain distribution in FSW operations. The model was calibrated with a basic benchmark of individual plates connected via an FSW technique. Three distinct single stiffener cross-section geometries were examined: a panel with a T stiffener geometry and two panels with blade stiffeners. The residual stress distribution was comparable across several panels, with the exception of the stiffener region. The distortion magnitude exhibited a similar pattern but varied in magnitude among panels with different cross-sections.

Another study by Paulo et al. [78] presented that the numerical analysis of the buckling behavior of stiffened panels welded using FSW demonstrated the effectiveness of various modeling approaches tested. The research examined various distributions of welding effects adjacent to transverse edges and determined that the distribution of residual stress or softened material did not significantly influence the final outcomes. The incorporation of work hardening properties, in contrast to a simple perfectly plastic relation, enhanced the collapse load, especially in panels exhibiting elevated collapse load/yield load ratios, contingent upon higher equivalent plastic strain levels. Two methodologies for modeling welding effects, namely FSW simulations and simplified modeling, exhibited differing results attributable to distinct initial geometrical imperfections. Initial geometrical imperfections significantly influenced the collapse loads and buckling modes of panels,

thereby affecting the residual welding effects. The presence of softened material in the welded zone of panels exhibiting similar collapse modes led to a reduction in collapse load. Residual stress fields in panels exhibiting similar collapse modes postpone the initial mode change during loading, while in the welded zone softened material enhanced the collapse load. Residual stresses and softened materials may influence the buckling modes in certain instances.

#### 5. Impact of manufacturing decisions of welding processes on the final structural behavior of ISP during service

The final structural behavior of ISP during service is largely determined by manufacturing decisions, especially those made in the welding operations. Characteristics of the weld joint, including strength, ductility, and dimensional accuracy, are influenced by the choice of welding process, heat input, and cooling rates. The structural integrity may be compromised by residual stresses and distortions following welding, which may result in fatigue, stress corrosion cracking, or early collapse under load [79]. Joints are weakened by defects like porosity or partial fusion, and material toughness is changed by microstructural alterations in the HAZ [80]. To guarantee weld quality and increase durability and service life, post-weld treatments and strict inspection procedures are necessary. Under operating conditions, dependable performance is ensured by proper control of these elements [81]. Furthermore, for FSW, Process parameters include welding traverse speed, rotational speed, tilt angle, shoulder profile, probe, and axial force must be optimized in order to a successful application of FSW [82].

#### 6. Conclusions

This study reveals that numerous numerical and experimental investigations have been conducted to predict the buckling load, fatigue life, and fatigue crack growth rate of ISP and to compare these results with those of conventionally stiffened panels. However, the methods and results have been not the same. Herein, buckling investigations have been carried out where the panels are compressively loaded axially considered. Both buckling and fatigue investigations have been only modeled and tested on the flat integral panel without a frame in the structure. In comparison to the riveted panel, the machined ISP has had a better compressive buckling load. However, due to residual stress, the FSW integral panel had a lower buckling load than the riveted panel. With respect to fatigue investigation, LFM based on SIF has been used to determine the magnitude of the local stress around the crack tip in FCP analysis. This factor is affected by various factors including the loading, the size and shape of the crack, and the boundaries of the geometric structure. Residual stress is influencing the fatigue life of ISP. Absences of residual stress, such as in machined stiffened panels, demonstrated a lower fatigue life. In opposition, the FSW panels have a higher fatigue life due to the residual compressive stress field in the middle of the panel that causes the crack growth rate to slow down. Similar to that, residual stress since LBW leads to a decline of the SIF values, reducing the growth of fatigue cracks. In comparison to riveted panels, integral stiffening causes a higher SIF and has a lower damage tolerance capability. Fatigue crack growth and buckling resistance in FSW and LBW are directly influenced by the weld's quality. Thus, to improve weld quality, structural integrity, and productivity, precise computational models, experimental methods, and welding parameter optimization are required. Further study is needed as follows:

1. It is known that the panel's curvature has an effect on its buckling and fatigue performance. The experiment by Weimin

- et al. [51] resulted in the buckling behavior of curved machined ISP. For further investigation, it is crucial to determine the buckling and fatigue performances for curved FSW ISP or curved LBW ISP containing frame to more represent the aircraft fuselage panel.
- The optimal buckling and fatigue behavior can also be affected by the geometry, shape, configuration, and dimensions of stringers and frames. The investigation by Caseiro et al. [55] exhibited the importance of optimization of the cross-section of ISP structure. Therefore, the design analysis of the stringer cross-section, shape, and configuration needs to be conducted to improve the buckling and fatigue behavior in integral structures.
  - The joining quality of FSW or LBW influences the buckling strength and crack growth rate of the panel. Optimization of FSW and LBW parameters and geometry could be done to increase weld quality and productivity.
  - To further improve the fatigue and buckling behavior of welded ISP, future research should concentrate on creating sophisticated design tools, reliable simulation models, and exhaustive experimental inspections.

### CRediT authorship contribution statement

**Devi Chandra:** Writing – original draft. **Y. Nukman:** Conceptualization. **Muhammad Adlan Azka:** Writing – original draft. **S.M. Sapuan:** Supervision. **J. Yusuf:** Writing – original draft.

### Declaration of competing interest

S. M. Sapuan is an editorial board member/editor-in-chief for Defence Technology and was not involved in the editorial review or the decision to publish this article. All authors declare that there are no competing interests.

### Acknowledgment

The authors express their gratitude to Universiti Pura Malaysia (UPM), Malaysia for granting Putra IPS vote number 9742900.

### References

- Beukers A, van Tooren M, Vermeeren C. Aircraft structures in the century ahead: from arts to science, from craftsmanship to multidisciplinary design and engineering. *Aeronaut J* 2003;107:343–57. <https://doi.org/10.1017/S0001924000013671>.
- Niemann S, Kolesnikov B, Lohse-Busch H, Hühne C, Querin OM, Toropov VV, et al. The use of topology optimization in the conceptual design of next generation lattice composite aircraft fuselage structures. *Aeronaut J* 2013;117:1139–54. <https://doi.org/10.1017/S0001924000008745>.
- Simmons MC, Schleyer GK. Pulse pressure loading of aircraft structural panels. *Thin-Walled Struct* 2006;44:496–506. <https://doi.org/10.1016/j.tws.2006.05.002>.
- Arcari A, Anderson RM, Hangarter CM, Iezzi EB, Policastro SA. Tensile properties of aircraft coating systems and applied strain modeling. *Coatings* 2024;14:91. <https://doi.org/10.3390/coatings14010091>.
- Zakar F. Multiple-site fatigue cracking of fuselage structure due to improper rivet installation. *J Fail Anal Prev* 2024;24:24–31. <https://doi.org/10.1007/s11668-023-01801-w>.
- Bhaumik SK, Sujata M, Venkataswamy MA. Fatigue failure of aircraft components. *Eng Fail Anal* 2008;15:675–94. <https://doi.org/10.1016/j.engfailanal.2007.10.001>.
- Zhang X, Li Y. Damage tolerance and fail safety of welded aircraft wing panels. *AIAA J* 2005;43:1613–23. <https://doi.org/10.2514/1.10275>.
- Boretti A. A techno-economic perspective on 3D printing for aerospace propulsion. *J Manuf Process* 2024;109:607–14. <https://doi.org/10.1016/j.jmapro.2023.12.044>.
- Najmon JC, Raesis S, Tovar A. Review of additive manufacturing technologies and applications in the aerospace industry. *Addit. Manuf. Aerosp. Ind.*, Elsevier 2019;7–31. <https://doi.org/10.1016/B978-0-12-814062-8.00002-9>.
- Zhu L, Li N, Childs PRN. Light-weighting in aerospace component and system design. *Propuls Power Res* 2018;7:103–19. <https://doi.org/10.1016/j.jprr.2018.04.001>.
- Williams JC, Starke EA. Progress in structural materials for aerospace systems. *Acta Mater* 2003;51:5775–99. <https://doi.org/10.1016/j.actamat.2003.08.023>.
- Fensin SJ, Dattelbaum DM, Jones DR, Gray GT. Dynamic behavior of additively manufactured materials. In: Hokka MBT-DB, of M, editors. *Dyn. Behav. Mater.* Elsevier; 2024. p. 411–48. <https://doi.org/10.1016/B978-0-323-99153-7.00012-8>.
- Hao P, Liu D, Liu H, Feng S, Wang B, Li G. Intelligent optimum design of large-scale gradual-stiffness stiffened panels via multi-level dimension reduction. *Comput Methods Appl Mech Eng* 2024;421:116759. <https://doi.org/10.1016/j.cma.2024.116759>.
- Alexopoulos ND, Gialos AA, Zeimpekis V, Velonaki Z, Kashaev N, Riekehr S, et al. Laser beam welded structures for a regional aircraft: weight, cost and carbon footprint savings. *J Manuf Syst* 2016;39:38–52. <https://doi.org/10.1016/j.jmsy.2016.02.002>.
- Dursun T, Soutis C. Recent developments in advanced aircraft aluminium alloys. *Mater Des* 2014;56:862–71. <https://doi.org/10.1016/j.matdes.2013.12.002>.
- Wang D, Xu F, Yuan L, Zhang D, Liu J, Hu Y, et al. Brief introduction and recent development on the manufacture of aluminium alloy integral panels in aerospace applications. *Int J Mater Struct Integr* 2021;14:299. <https://doi.org/10.1504/IJMSI.2021.125814>.
- Zain-ul-abdein M, Nélias D, Jullien J-F, Deloison D. Experimental investigation and finite element simulation of laser beam welding induced residual stresses and distortions in thin sheets of AA 6056-T4. *Mater Sci Eng A* 2010;527:3025–39. <https://doi.org/10.1016/j.msea.2010.01.054>.
- Daneshpour S, Koçak M, Langlade S, Horstmann M. Effect of overload on fatigue retardation of aerospace Al-alloy laser welds using crack-tip plasticity analysis. *Int J Fatigue* 2009;31:1603–12. <https://doi.org/10.1016/j.ijfatigue.2009.04.005>.
- Schubert E, Klassen M, Zerner I, Walz C, Sepold G. Light-weight structures produced by laser beam joining for future applications in automobile and aerospace industry. *J Mater Process Technol* 2001;115:2–8. [https://doi.org/10.1016/S0924-0136\(01\)00756-7](https://doi.org/10.1016/S0924-0136(01)00756-7).
- Skillingberg M, Green J. Aluminum applications in the rail industry. *Light Met Age* 2007;65:8.
- Çam G, Mistikoglu S. Recent developments in friction stir welding of Al-alloys. *J Mater Eng Perform* 2014;23:1936–53. <https://doi.org/10.1007/s11665-014-0968-x>.
- Burford DA. Friction stir welding of airframe structure: from one delivery system to another. *SAE Tech. Pap.* 2003. <https://doi.org/10.4271/2003-01-2897>.
- Rajendran C, Srinivasan K, Balasubramanian V, Sonar T, Balaji H. Friction stir welding for manufacturing of a light weight combat aircraft structure. *Mater Test* 2022;64:1782–95. <https://doi.org/10.1515/mt-2022-0165>.
- Mendez PF, Eagar TW. Welding processes for aeronautics. *Adv Mater Process* 2001;159:39–43.
- Kallee SW. Industrial applications of friction stir welding. *Frict. Stir Weld.*, Elsevier 2010:118–63. <https://doi.org/10.1533/9781845697716.1.118>.
- Majeed T, Wahid MA, Alam MN, Mehta Y, Siddiquee AN. Friction stir welding: a sustainable manufacturing process. *Mater Today Proc* 2021;46:6558–63. <https://doi.org/10.1016/j.matpr.2021.04.025>.
- Shtrikman MM. Current state and development of friction stir welding Part 3. Industrial application of friction stir welding. *Weld Int* 2008;22:806–15. <https://doi.org/10.1080/09507110802593620>.
- Maciel R, Infante V, Braga D, Moreira P, Bento T, da Silva L. Development of hybrid friction stir welding and adhesive bonding single lap joints in aluminium alloys. *Frat Ed Integrità Strutt* 2019;13:269–85. <https://doi.org/10.3221/IGF-ESIS.48.28>.
- Ahmed MMZ, El-Sayed Seleman MM, Fydrich D, Çam G. Friction stir welding of aluminum in the aerospace industry: the current progress and state-of-the-art review. *Materials* 2023;16:2971. <https://doi.org/10.3390/ma16082971>.
- Campbell Jr FC. *Manufacturing technology for aerospace structural materials.* Elsevier; 2011.
- Zheng K, Politis DJ, Wang L, Lin J. A review on forming techniques for manufacturing lightweight complex-shaped aluminium panel components. *Int J Light Mater Manuf* 2018;1:55–80. <https://doi.org/10.1016/j.ijlmm.2018.03.006>.
- Echraf SBM, Hrairi M. Research and progress in incremental sheet forming processes. *Mater Manuf Process* 2011;26:1404–14. <https://doi.org/10.1080/10426914.2010.544817>.
- Bains PS, Sidhu SS, Payal HS. Fabrication and machining of metal matrix composites: a review. *Mater Manuf Process* 2016;31:553–73. <https://doi.org/10.1080/10426914.2015.1025976>.
- Quinn D, Murphy A, McEwan W, Lemaitre F. Stiffened panel stability behaviour and performance gains with plate prismatic sub-stiffening. *Thin-Walled Struct* 2009;47:1457–68. <https://doi.org/10.1016/j.tws.2009.07.004>.
- Wilson R, Murphy A, Price MA, Glazebrook C. A preliminary structural design procedure for laser beam welded airframe stiffened panels. *Thin-Walled Struct* 2012;55:37–50. <https://doi.org/10.1016/j.tws.2012.03.003>.
- Ion JC. Laser beam welding of wrought aluminium alloys. *Sci Technol Weld Join* 2000;5:265–76. <https://doi.org/10.1179/136217100101538308>.
- Bunaziv I, Akselsen OM, Ren X, Nyhus B, Eriksson M. Laser beam and laser-arc hybrid welding of aluminium alloys. *Metals* 2021;11:1150. <https://doi.org/10.3390/met11081150>.

- [38] Dittrich D, Standfuss J, Liebscher J, Brenner B, Beyer E. Laser beam welding of hard to weld Al alloys for a regional aircraft fuselage design – first results. *Phys Procedia* 2011;12:113–22. <https://doi.org/10.1016/j.phpro.2011.03.015>.
- [39] Xiao R, Zhang X. Problems and issues in laser beam welding of aluminum–lithium alloys. *J Manuf Process* 2014;16:166–75. <https://doi.org/10.1016/j.jmapro.2013.10.005>.
- [40] Sun Z, Ion JC. Laser welding of dissimilar metal combinations. *J Mater Sci* 1995;30:4205–14. <https://doi.org/10.1007/BF00361499>.
- [41] Hilburger M. Developing the next generation shell buckling design factors and technologies. 53rd AIAA/ASME/ASCE/AHS/ASC Struct. Struct. Dyn. Mater. Conf. AIAA/ASME/AHS Adapt. Struct. Conf. AIAA. Reston, Virginia: American Institute of Aeronautics and Astronautics; 2012. p. 1686. <https://doi.org/10.2514/6.2012-1686>.
- [42] Datta PK, Biswas S. Research advances on tension buckling behaviour of aerospace structures: a review. *Int J Aeronaut Sp Sci* 2011;12:1–15. <https://doi.org/10.5139/IJASS.2011.12.1.1>.
- [43] Sreenivasa R, Kallesh SS, Naveen Kumar KHSSH. Study the effect of buckling on aircraft fuselage skin panel with or without airframe, vol. 1; 2016. p. 346–53.
- [44] Young R, Rose C, Starnes Jr K. Skin, stringer, and fastener loads in buckled fuselage panels. 19th AIAA appl. Aerodyn. Conf. Reston, Virginia: American Institute of Aeronautics and Astronautics; 2001. <https://doi.org/10.2514/6.2001-1326>.
- [45] Kolchuzhin V, Mehner JE, Gessner T, Doetzel W. Parametric finite element analysis for reduced order modeling of MEMS. EuroSime 2006 - 7th Int. Conf. Therm. Mech. Multiphysics Simul. Exp. Micro-Electronics Micro-Systems 2006;2006:1–6. <https://doi.org/10.1109/ESIME.2006.1644004>. IEEE.
- [46] Aalberg A, Langseth M, Larsen P. Stiffened aluminium panels subjected to axial compression. *Thin-Walled Struct* 2001;39:861–85. [https://doi.org/10.1016/S0263-8231\(01\)00021-0](https://doi.org/10.1016/S0263-8231(01)00021-0).
- [47] Hoffman EK, Hafley RA, Wagner JA, Jegley DC, Pecquet RW, Blum CM, et al. Compression buckling behavior of large-scale friction stir welded and riveted 2090-T83 Al-Li alloy skin-stiffener panels. *NASA Langley Res Cent* 2002.
- [48] Majeed T, Mehta Y, Siddiquee AN. Challenges in joining of unequal thickness materials for aerospace applications: a review. *Proc Inst Mech Eng Part L J Mater Des Appl* 2021;235:934–45. <https://doi.org/10.1177/1464420720978682>.
- [49] Murphy A, Lynch F, Price M, Wang P. The static strength analysis of friction stir welded stiffened panels for primary fuselage structure. *Proc Int Council Aeronaut Sci ICAS 2004* 2004.
- [50] Murphy A, McCune W, Quinn D, Price M. The characterization of friction stir welding process effects on stiffened panel buckling performance. *Thin-Walled Struct* 2007;45:339–51. <https://doi.org/10.1016/j.tws.2007.02.007>.
- [51] Sun W, Tong M, Guo L, Dong D. Post-buckling simulation of an integral aluminum fuselage panel subjected to axial compression load. *Asia Simul. Conf. - 7th Int. Conf. Syst. Simul. Sci. Comput.* 2008:893–7. <https://doi.org/10.1109/ASC-ICSC.2008.4675489>. IEEE; 2008.
- [52] Yoon JW, Bray GH, Valente RAF, Childs TER. Buckling analysis for an integrally stiffened panel structure with a friction stir weld. *Thin-Walled Struct* 2009;47:1608–22. <https://doi.org/10.1016/j.tws.2009.05.003>.
- [53] Khedmati MR, Zareei MR, Rigo P. Sensitivity analysis on the elastic buckling and ultimate strength of continuous stiffened aluminium plates under combined in-plane compression and lateral pressure. *Thin-Walled Struct* 2009;47:1232–45. <https://doi.org/10.1016/j.tws.2009.04.010>.
- [54] Neto EL, Monteiro F A C, Ruela HH. A comparison of buckling performance of rivet and friction stir welding stiffened panels. *Mecánica Comput* 2010;XXIX:4967–75.
- [55] Caseiro JF, Valente RAF, Andrade-Campos A, Yoon JW. On an innovative optimization approach for the design of cross-section profiles of integrally stiffened panels subjected to elasto-plastic buckling deformation modes. *Int J Mater Form* 2010;3:49–52. <https://doi.org/10.1007/s12289-010-0704-5>.
- [56] Shah J, Gibson A, Price M. An investigation into the effects of experimental errors on the correlation between FEA and test results for a welded fuselage panel. *ICAS; 2002* 2002.
- [57] Noorsuhada MN. An overview on fatigue damage assessment of reinforced concrete structures with the aid of acoustic emission technique. *Constr Build Mater* 2016;112:424–39. <https://doi.org/10.1016/j.conbuildmat.2016.02.206>.
- [58] Vasudevan AK, Sadananda K, Iyyer N. Fatigue damage analysis: issues and challenges. *Int J Fatigue* 2016;82:120–33.
- [59] Li X, Zhou C, Xing C, He A, Yu J, Wang G. A phase-field fracture model for fatigue behavior in fiber-reinforced composites. *Int J Mech Sci* 2024;269:108989. <https://doi.org/10.1016/j.ijmecsci.2024.108989>.
- [60] Chudnovsky A. Slow crack growth, its modeling and crack-layer approach: a review. *Int J Eng Sci* 2014;83:6–41. <https://doi.org/10.1016/j.ijengsci.2014.05.015>.
- [61] Newman JC. *Advances in fatigue and fracture mechanics analyses for aircraft structures*. NASA Langley Res Cent; 1999.
- [62] Munroe J, Wilkins K, Gruber M, Domack MS. *Integral Airframe Structures (IAS): validated feasibility study of integrally stiffened metallic fuselage panels for reducing manufacturing costs*. Tech Rep NASA/CR-2000-209337 2000.
- [63] Murphy A, Quinn DQ, Mawhinney P, Ozacka M, van der Veen S. Tailoring static strength performance of metallic stiffened panels by selective local sub-stiffening. 47th AIAA/ASME/ASCE/AHS/ASC Struct. Struct. Dyn. Mater. Conf. 14th AIAA/ASME/AHS Adapt. Struct. Conf. 7th 2006;6:4339–54. <https://doi.org/10.2514/6.2006-1944>. Reston, Virginia: American Institute of Aeronautics and Astronautics.
- [64] Brot A, Peleg-Wolfin Y, Kressel I, Yosef Z. The damage-tolerance behavior of integrally stiffened metallic structures. 48th isr annu conf aerosp sci IACAS conf. 2008.
- [65] Merati A, Gallant M, Dubourg L, Jahazi M. Friction stir lap welding of AA 7075-T6 stringers on AA 2024-T3 skin. *ASM Proc. Int. Conf. Trends Weld. Res.* 2009:781–7. <https://doi.org/10.1361/cp2008twr781>.
- [66] Llopert L, Kurz B, Wellhausen C, Anglada M, Drechsler K, Wolf K. Investigation of fatigue crack growth and crack turning on integral stiffened structures under mode I loading. *Eng Fract Mech* 2006;73:2139–52. <https://doi.org/10.1016/j.engfracmech.2006.04.005>.
- [67] Castro PMS, Tavares SMO, Matos PFP De, Moreira PMGP. Damage tolerance of aircraft panels. *Mecánica Exp* 2010;18:35–46.
- [68] Tavares SMO, Richter-trummer V, Moreira PMGP, de Castro P, Castro MST De, Models CG, et al. Fatigue behavior of lightweight integral panels. 7th EURO-MECH solid mech conf. 2009.
- [69] Labeas G, Diamantakos I, Kermanidis T. Assessing the effect of residual stresses on the fatigue behavior of integrally stiffened structures. *Theor Appl Fract Mech* 2009;51:95–101. <https://doi.org/10.1016/j.tafmec.2009.04.003>.
- [70] Nesterenko GI. Comparison of damage tolerance of integrally stiffened and riveted structures. *Proc 22nd Int Council Aeronaut Sci* 2000.
- [71] Adeel M. Study on damage tolerance behavior of integrally stiffened panel and conventional stiffened panel. *World Acad Sci Eng Technol* 2008;45:1026–30. <https://doi.org/10.5281/zenodo.1328684>.
- [72] Uz M-V, Koçak M, Lemaitre F, Ehrström J-C, Kempa S, Bron F. Improvement of damage tolerance of laser beam welded stiffened panels for airframes via local engineering. *Int J Fatigue* 2009;31:916–26. <https://doi.org/10.1016/j.ijfatigue.2008.10.003>.
- [73] Augustin P. Simulation of fatigue crack growth in integrally stiffened panels under the constant amplitude and spectrum loadin. *Fatigue Aircr Struct* 2009;2009:5–19. <https://doi.org/10.2478/v10164-010-0001-2>.
- [74] Lemmen HJK, Alderliesten RC, Benedictus R. Fatigue initiation behaviour throughout friction stir welded joints in AA2024-T3. *Int J Fatigue* 2010;32:1928–36. <https://doi.org/10.1016/j.ijfatigue.2010.06.001>.
- [75] Paulo RMF, Teixeira-Dias F, Valente RAF. Numerical simulation of aluminium stiffened panels subjected to axial compression: sensitivity analyses to initial geometrical imperfections and material properties. *Thin-Walled Struct* 2013;62:65–74. <https://doi.org/10.1016/j.tws.2012.07.024>.
- [76] Paulo RMF, Carlone P, Valente RAF, Teixeira-Dias F, Palazzo GS. Influence of friction stir welding residual stresses on the compressive strength of aluminium alloy plates. *Thin-Walled Struct* 2014;74:184–90. <https://doi.org/10.1016/j.tws.2013.09.012>.
- [77] Paulo RMF, Carlone P, Paradiso V, Valente RAF, Teixeira-Dias F. Prediction of friction stir welding effects on AA2024-T3 plates and stiffened panels using a shell-based finite element model. *Thin-Walled Struct* 2017;120:297–306. <https://doi.org/10.1016/j.tws.2017.09.009>.
- [78] Paulo RMF, Rubino F, Valente RAF, Teixeira-Dias F, Carlone P. Modelling of friction stir welding and its influence on the structural behaviour of aluminium stiffened panels. *Thin-Walled Struct* 2020;157:107128. <https://doi.org/10.1016/j.tws.2020.107128>.
- [79] den Besten H. Fatigue damage criteria classification, modelling developments and trends for welded joints in marine structures. *Ships Offshore Struct* 2018;13:787–808.
- [80] Nazemi N. Identification of the mechanical properties in the heat-affected zone of aluminum welded structures. 2015.
- [81] Wang B, Hu SJ, Sun L, Freiheit T. Intelligent welding system technologies: state-of-the-art review and perspectives. *J Manuf Syst* 2020;56:373–91.
- [82] Gite RA, Loharkar PK, Shimpi R. Friction stir welding parameters and application: a review. *Mater Today Proc* 2019;19:361–5. <https://doi.org/10.1016/j.matpr.2019.07.613>.